ELSEVIER

Surface Science 373 (1997) 230–236

surface science

Dirac δ nucleation in the framework of Avrami's model: the case of diamond growth on deformed Si(100)

R. Polini [a,*], M. Tomellini [a], M. Fanfoni [b], F. Le Normand [c]

[a] *Università di Roma "Tor Vergata", Dipartimento di Scienze e Tecnologie Chimiche, Via della Ricerca Scientifica, 00133 Roma, Italy*

[b] *Università di Roma "Tor Vergata", Dipartimento di Fisica and Istituto Nazionale di Fisica della Materia, Via della Ricerca Scientifica, 00133 Roma, Italy*

[c] *Groupe Surfaces–Interfaces, IPCMS, UMR 046 du CNRS, Bâtiment 69, 23 rue du Loess, 67037 Strasbourg Cedex, France*

Received 22 May 1996; accepted for publication 3 September 1996

Abstract

The nucleation and growth kinetics of diamond deposited by hot-filament chemical vapour deposition (HFCVD) on Si(100) substrates, previously deformed by uniaxial compression along the ⟨100⟩ direction, have been investigated. Although the nucleation density at saturation (0.04–0.06 μm^{-2}) was similar to those measured on virgin, as-received Si(100) wafers, the kinetics of stable nucleus formation resembled the fast kinetics observed for substrates which were mechanically abraded prior to CVD in order to enhance diamond nucleation. The results definitely indicate that diamond nucleation occurs randomly with a rate that is a Dirac δ function. The time dependence of the substrate fraction which is covered by islands was measured, and a good agreement with Avrami's kinetics for 2D phase transitions was found. The total island perimeter has also been measured as a function of the covered surface, and is well described by the analytical model recently developed [M. Tomellini and M. Fanfoni, Surf. Sci. 349 (1996) L191]. The observed fast nucleation has been attributed to stress-induced defects pre-existing at the surface and which provides suitable sites for diamond growth.

Keywords: Chemical vapor deposition; Diamond; Growth; Nucleation; Polycrystalline thin films; Scanning electron microscopy (SEM); Silicon

1. Introduction

In the past decade, several chemical vapour deposition (CVD) processes have been developed for the production of high-quality diamond coatings on substrates as different as metals, semiconductors and ceramics. The success in growing diamond thin films using CVD methods has stimulated an enormous interest in the unique combination of properties of diamond for new technological applications [1].

Diamond-film formation on non-diamond substrates occurs via the Volmer–Weber growth mode [2], since diamond has the highest surface energies of any known material. In most CVD methods, heterogeneous diamond nucleation is a demanding process which requires the presence of suitable nucleation sites at the substrate surface, whose nature is still controversial [3]. As a matter of fact, diamond nucleation on untreated surfaces is usually both very difficult and slow. A recent detailed investigation on the diamond nucleation

*Corresponding author. Fax: +39 6 72594328; e-mail: polini@utovrm.it

0039-6028/97/$17.00
PII S0039-6028(96)01158-2

kinetics at the surface of as-received Si(100) wafers found that the density of diamond nuclei formed under CVD conditions similar to those employed in this work reached a value of 0.027 μm^{-2} after more than 10 h of deposition, without reaching saturation [4]. On Si(100) substrates scratched with abrasive powders or pretreated by ultrasonic agitation with diamond powder, much higher nucleation densities ($>1\ \mu m^{-2}$) are commonly obtained in less than 1 h of deposition [5–7]. In recent years, a number of nucleation-enhancement methods have been developed which allow the control of nucleation density over several orders of magnitude [8–19]. This is an important achievement, since the nucleation process critically determines film's properties as well as its morphology and adhesion. Although the experimental investigations have contributed significantly to develop technologies for optical and electronic applications and for the production of wear-resistant components in the cutting-tool and metal-working industries, it is evident from the literature that a clear picture of diamond nucleation in CVD is still needed to provide insight into the nucleation kinetics [3].

In this paper we report a study on diamond formation on Si(100) which was plastically deformed, prior to deposition, by uniaxial compression. Such a deformation procedure allows us to control the dislocation density in the crystal. The kinetics of nucleation as well as the time dependence of the surface fraction covered by islands have been determined. Moreover, for the first time, the evolution of the total island perimeter has been measured and its behaviour, as a function of the covered surface fraction, has been analysed on the basis of a recently developed kinetic model [20].

2. Experimental

Si(100) (electronic grade) was supplied by Wacker and was purified by the melting-zone method. The impurity levels for carbon and oxygen were 5×10^{15} and 10^{16} atoms cm^{-3}, respectively. The silicon was slightly n-doped with phosphorous (10^{15} atoms cm^{-3}). Stable plastic deformation was created by uniaxial compression along the $\langle 110\rangle$ direction at 1100°C in an inert atmosphere (90% He + 10% H_2). The deformation rate was $3.5\times10^{-4}\ s^{-1}$. The resulting dislocation density was $1.5\pm0.5\times10^{8}\ cm^{-1}$, as measured by transmission electron microscopy. The silicon was then cut with a diamond saw according to the (100) orientation (±2°). The wafers were mechanically polished with 0.25 μm diamond paste and their surfaces were cleaned with boiled trichloroethylene and finally chemically etched with a solution of 32.5% HNO_3 + 17.5% HF and 50% acetone for 2 min. This treatment ensures the removal of the stress-hardened layer (about 20 μm). Prior to deposition, the 10 mm × 5 mm samples were rinsed with deionised water and treated in an ultrasonic bath with ethanol.

Diamond synthesis was performed in a conventional stainless steel hot-filament chemical vapor deposition (HFCVD) chamber. The gas phase, a mixture of hydrogen (purity 99.9990%) and methane (purity 99.995%) with a $CH_4:H_2$ volume ratio fixed at 0.5%, was activated by a hot tantalum filament (0.03 cm in diameter) wound in a 0.14 cm internal diameter spiral and accurately positioned by means of a cathetometer at 0.8 cm from the substrate. The filament temperature (2100°C) was monitored by a two-colour optical pyrometer (LAND INFRARED model RP 12). The power dissipated by the filament was in the range 140–160 W. A new filament was used in each deposition run. The total pressure of the gas mixture in the reactor was 23 Torr, with a total flow rate of 200 sccm. Gas composition and flow rates were set up by digital mass flow controllers (MKS model 258/259). The substrate temperature (800°C) was measured by a Pt/Pt–Rh10% thermocouple pressed against the heated molybdenum ribbon supporting the sample. Deposition times were varied between 0.5 and 10.5 h. Following deposition, all the samples were analyzed by scanning electron microscopy (SEM, Leica Cambridge model Stereoscan 360). The SEM pictures were processed by Automatic Image Analysis (AIA, Cambridge Instruments Quantimet 970) in order to measure the substrate area fraction covered by diamond, $S(t)$, and the total perimeter of the deposit per unit area, $P(t)$. In the case of samples deposited for less than 7 h, the deposit was consti-

tuted by well-separated particles and it was possible to count the nucleation density (nuclei per unit area) and measure the size distribution function of diamond crystallites. Equivalent diameter $d=(4A/\pi)^{1/2}$, where A is the projected area in μm^2 of diamond crystallites, was used as a size parameter.

Raman spectroscopy confirmed that diamond was the main component of the deposits.

3. Results and discussion

In Table 1 the deposition times and the AIA results are summarized. These results will be considered and discussed in detail below.

In Fig. 1 SEM pictures of samples 2, 3, 4 and 6 are shown. These micrographs clearly show that, at a given deposition time t_D, the diamond crystallites are of nearly the same size, and that for $t_D \leqslant 5$ h the deposits consist of well-separated particles. The particle-size distribution functions, $F(d,t_D)$ of samples 2–4, where particle impingement is negligible, are plotted in Fig. 2 and indicate that, as the deposition time increases, the $F(d,t_D)$ moves towards higher diameter values while its width remains practically constant. In Fig. 3 the time evolutions of both maximum (d_{max}) and average ($\langle d \rangle$) diameters of crystallites are reported. These quantities increase linearly in time with constant rates of 0.7 $\mu m\ h^{-1}$ and 0.6 $\mu m\ h^{-1}$, respectively. The growth rate is therefore controlled by reactions occurring at the surface of the growing diamond particles [21], and no concentration gradient of gas-phase precursors (H, CH_3 and C_2H_2) develops between the bulk of the activated gas and the gas–solid interface [22,23]. The reason for using d_{max} as a growth parameter has been explained elsewhere [22]. We recall that the growth time of a diamond particle of diameter d in the size distribution is $t_g=t_D[d/d_{max}(t_D)]$. The growth time of the biggest particles can be assumed to be equal to the deposition time, t_D, while the growth times of the smaller particles are lower than t_D. The small difference between d_{max} and $\langle d \rangle$ stems from the small width of the size distribution functions.

According to the procedure reported in Refs. [24–26], the nucleation kinetics, $N(t)$, can be calculated by using the temporal evolution of d_{max} and the $F(d,t_D)$ functions of Fig. 2. The results are shown in Fig. 4, and definitely indicate that the nucleation stage ends in less than 1 h of deposition when the surface fraction covered by diamond is less than 2% (Table 1). In other words, the time required for nucleation to reach completion ($t_D < 1$ h) is negligible compared to the time necessary for film formation ($t_D > 10.5$ h, $S(10.5)=91\%$). The same conclusion could be drawn by considering the measured nucleation densities reported in Table 1. From this analysis we infer that the diamond nucleation rate goes to zero at the very beginning of film formation. Therefore, the nucleation rate can be modelled as a Dirac δ function [20], i.e. all nuclei start growing simultaneously. It is worth noticing that the nucleation rates on Si(100) substrates which were mechanically

Table 1
Deposition times and diamond-growth parameters determined by digital processing of SEM pictures

Sample	Deposition time (h)	Maximum diameter (μm)	Average diameter (μm)	Nucleation density (μm^{-2})	Surface coverage, $S(t)$	Perimeter, $P(t)$ (μm^{-1})
1	0.5	0.5	0.4	0.033 ± 0.018	0.0048 ± 0.0029	0.051 ± 0.030
2	1	0.75	0.6	0.057 ± 0.022	0.0181 ± 0.007	0.124 ± 0.049
3	3	2.4	1.9	0.046 ± 0.007	0.140 ± 0.023	0.284 ± 0.056
4	5	3.1	2.8	0.036 ± 0.005	0.257 ± 0.016	0.309 ± 0.013
5	5+0.5	3.7	3.3	—	0.346 ± 0.042	0.363 ± 0.021
6	6	5.1	4.3	0.044 ± 0.005	0.591 ± 0.09	0.318 ± 0.052
7	7	—	—	—	0.808 ± 0.042	0.266 ± 0.033
8	3+4	4.7	4.3	—	0.698 ± 0.134	0.330 ± 0.056
9	10.5	—	—	—	0.914 ± 0.018	0.089 ± 0.002

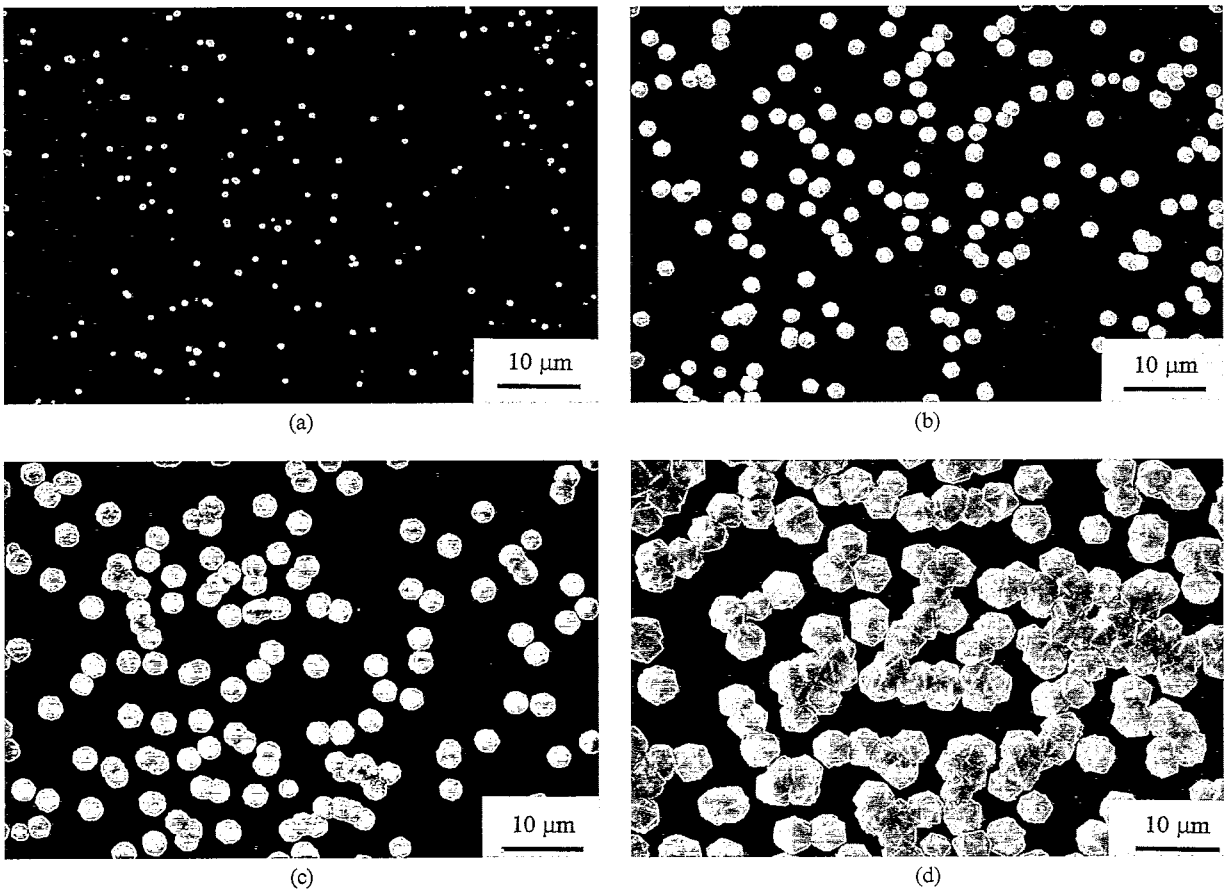

Fig. 1. SEM pictures of diamond deposits grown on deformed Si(100) for (a) 1 h (sample 2), (b) 3 h (sample 3), (c) 5 h (sample 4), and (d) 6 h (sample 6).

abraded prior to deposition exhibited a quite different behaviour [5,6]. In fact, in these cases we have measured nucleation rates different from zero up to 40–50% of surface coverage, and consequently the nucleation rate could not be described by a Dirac δ function.

In Fig. 5 the measured $S(t)$ kinetics is reported in the form $\ln\{-\ln[1-S(t)]\}$ versus $\ln(t)$. The data are well described by a straight line, which implies $S(t)=1-\exp(-kt^n)$, namely a stretched exponential function with $k=1.4\times10^{-9}\ \mathrm{s}^{-n}$ and $n=2.08$. It is worth recalling that in the case of Dirac δ nucleation, Avrami's kinetics leads to a stretched exponential function with n related to the growth law of the nuclei [27]. In particular, for a growth law in the form $d\propto t^m$, d being the diameter of the nucleus, $n/m=2$. Notably, from the independent measurements of $d(t)$ (Fig. 3) and $S(t)$ (Fig. 5), we get $n/m=2.08$. It is important to stress that Avrami's kinetics holds for a random distribution of nuclei. In order to check whether or not diamond nuclei are randomly distributed at the substrate surface, a statistical analysis has been performed on the ground of the Poisson distribution. For this purpose, we have counted the particles whose centers lie in the circle centered on each nucleus in the SEM pictures. We have chosen a disk of radius equal to the average distance between two particles, namely $1/\sqrt{N}$, N being the nucleation density in $\mu\mathrm{m}^{-2}$. The frequency of finding n particles in the sampling disk as a function of n is shown in Fig. 6 for sample 3, where

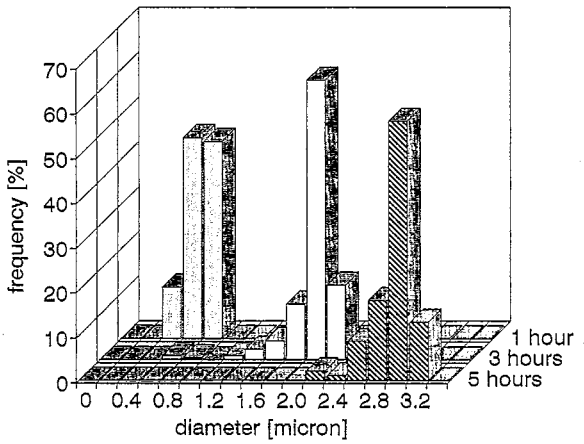

Fig. 2. Particle size distributions of diamond crystallites formed after 1, 3 and 5 h of deposition (samples 2, 3 and 4, respectively).

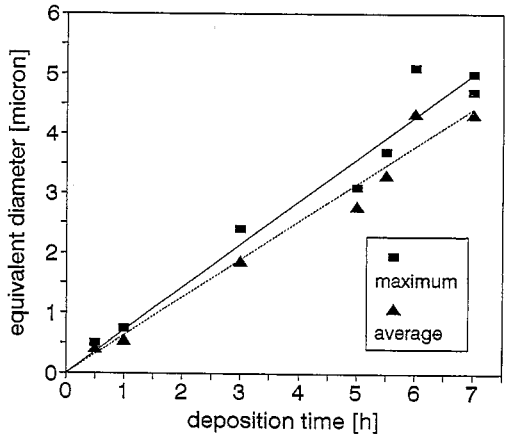

Fig. 3. Microscopic growth law of both the maximum, d_{max}, and the average, $\langle d \rangle$, equivalent diameter of diamond crystallites, as obtained from the size distribution functions of well-separated particles. Solid and dotted lines are the linear best fit to $d_{max}(t)$ and $\langle d(t) \rangle$ data, respectively.

274 independent measurements were considered. The full line is the Poisson function computed using the average n value, as obtained from particle counting. The reliability of the Poisson distribution has been confirmed by a χ^2 test, for which the threshold of probability to reject the hypothesis was found to be greater than 30%. This analysis confirms that diamond nuclei are formed at random on the surface of deformed Si(100) and, consequently, Avrami's prescriptions hold.

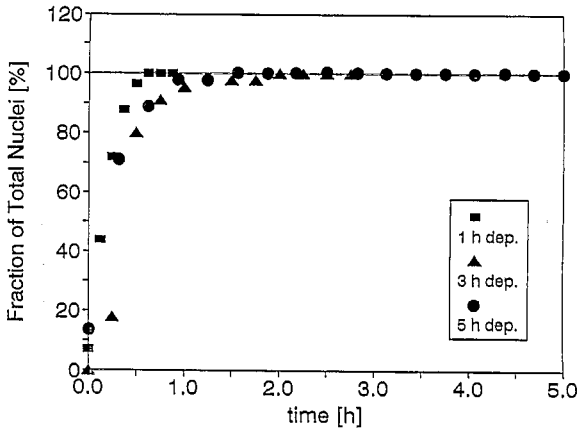

Fig. 4. Nucleation kinetics, $N(t)$, of diamond as derived from the particle size distributions of Fig. 2 and the $d_{max}(t)$ growth law reported in Fig. 3.

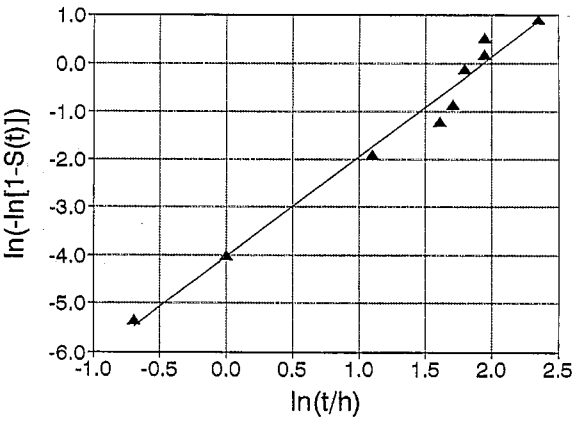

Fig. 5. Kinetics of the surface fraction, $S(t)$, covered by diamond islands in the form $\ln(-\ln[1-S(t)])$ versus $\ln(t)$.

In a recent paper [20] the kinetics of the total perimeter of the deposit has been modelled on the basis of Avrami's theory. For Dirac δ nucleation it was demonstrated that the total perimeter per unit area is a function of the surface coverage and does not depend on the growth law of the nuclei. The following analytical expression was obtained:

$$P(S) = \sqrt{4\pi N}(1-S)\left\{\ln\left[\frac{1}{1-S}\right]\right\}^{1/2}, \qquad (1)$$

where $P(S)$ is the perimeter per unit area, S is the surface fraction covered by the deposit, and N is the surface density of nuclei. According to Eq. (1),

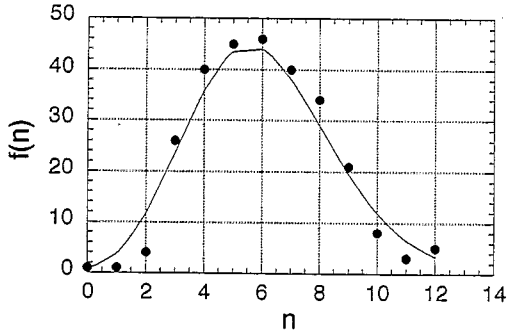

Fig. 6. Number of fields of observation containing n particles counted in a sampling disk, whose radius is equal to the average distance between two nuclei (sample 3, 3 h deposition). The solid line is the Poisson function evaluated using the mean value of particles in the sampling disk and obtained from the 274 independent observations.

the perimeter is maximum for $S=1-e^{-1/2}\cong 0.39$. In Fig. 7 the measured perimeter of the diamond deposit as a function of S is reported. The solid line is the best fit of Eq. (1) to the experimental data. From the fit we received $N=0.059\ \mu m^{-2}$, a value which is in good agreement with the measured nucleation densities of Table 1.

Hirakuri et al. [28] found that the diamond nucleation density on a Si(100) wafer mechanically stressed with a spring and a rod during CVD at 800°C was affected by the applied compressive stress. They measured nucleation densities up to about $0.5\ \mu m^{-2}$, i.e. several orders of magnitude higher than those reported in the literature for untreated Si(100) [3]. Unfortunately, no kinetic study was reported in Ref. [28]. Dennig and Stevenson [17] found that the nucleation of diamond from the gas phase in the HFCVD is promoted by topographical features, i.e. locations which protrude from the substrate surface, such as edges or apexes. Selective diamond nucleation has also been observed at steps of cleaved Si(111) surface [29]. In the case of deformed Si(100), both the high dislocation density and the surface asperities formed by the treatment employed to create linear defects could provide suitable sites for the observed fast nucleation process, but further work is required to clarify the nature of nucleation sites. Nevertheless, the system investigated here represents an ideal case for corroborating Avrami's theory and modelling thin-film growth when the nucleation rate can be approximated by Dirac δ function.

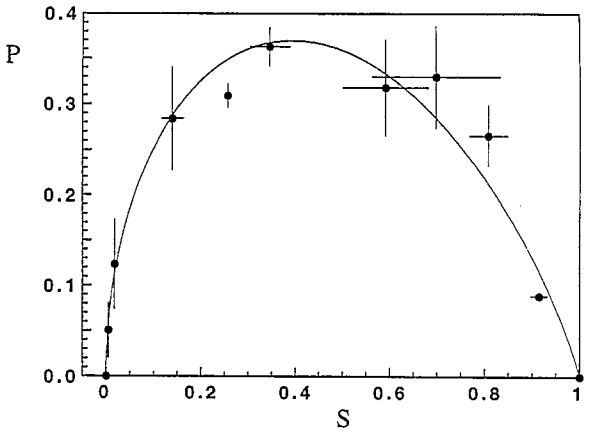

Fig. 7. Total perimeter of diamond deposit, P, as a function of the substrate coverage, S. The solid line is the best fit to the data using Eq. (1).

4. Conclusions

Diamond nucleation occurs at random on Si(100) substrates plastically deformed by uniaxial compression along the ⟨100⟩ direction, and reaches completion at very low values of substrate coverage (<2%). This occurrence allows one to consider the nucleation rate as a Dirac δ function. Although the nucleation density at saturation ($0.04–0.06\ \mu m^{-2}$) is only slightly higher than or equal to those measured on untreated Si(100) wafers, the kinetics of stable nucleus formation resembles the fast kinetics observed for scratched or ultrasonically pretreated substrates. These experimental evidences suggest that stress-induced defects produced by the thermomechanical treatment provides suitable sites for diamond nucleation at 800°C.

The time evolution of the covered surface is very well described by Avrami's theory. Moreover, we have also obtained the density of nuclei by measuring the total perimeter evolution as a function of surface coverage and fitting the data according to a recently developed model. This approach can be applied to other systems, such as the growth of

metal films on either semiconductor or metal substrates where the nucleation rate is usually a Dirac δ function [30–32].

Acknowledgements

We thank S. Choux and Professor J.P. Michel (Laboratoire de Métallurgie Physique, Ecole des Mines, Nancy, France) for supplying the silicon samples. This work was partially supported by the French Foreign Affairs Ministry and the Italian MURST, in the framework of "Programma Galileo".

References

[1] K.E. Spear and J.P. Dismukes (Eds.), Synthetic Diamond: Emerging CVD Science and Technology (Wiley, New York, 1994).
[2] M. Volmer and A. Weber, Z. Phys. Chem. 119 (1926) 277.
[3] H. Liu and D.S. Dandy, Diamond Relat. Mater. 4 (1995) 1173.
[4] L. Demuynck, Ph.D. Thesis, Université Louis Pasteur de Strasbourg, 1995.
[5] E. Molinari, R. Polini, V. Sessa, M.L. Terranova and M. Tomellini, J. Mater. Res. 8 (1993) 785.
[6] F. Le Normand, J.C. Arnault, L. Fayette, B. Marcus, M. Mermoux and V. Parasote, J. Appl. Phys. 80 (1996) 1830.
[7] R.A. Bauer, N.M. Sbrockey and W.E. Brower, Jr., J. Mater. Res. 8 (1993) 2858.
[8] S. Yugo, T. Kanai, T. Kimura and T. Muto, Appl. Phys. Lett. 58 (1991) 1036.
[9] X. Jiang, K. Schiffmann, A. Westphal and C.-P. Klages, Appl. Phys. Lett. 71 (1992) 5353.
[10] X. Jiang, K. Schiffmann and C.-P. Klages, Phys. Rev. B 50 (1994) 8402.
[11] K. Tamaki, Y. Watanabe, Y. Nakamura and S. Hirayama, Thin Solid Films 236 (1993) 115.
[12] D. Kim, H. Lee and J. Lee, J. Mater. Sci. 28 (1993) 6704.
[13] W.R.L. Lambrecht, C.H. Lee, B. Segall, J.C. Angus, Z. Li and M. Sunkara, Nature 364 (1993) 607.
[14] J. Singh and M. Vellaikal, J. Appl. Phys. 73 (1993) 2831.
[15] P. Bou, L. Vandenbulcke, R. Herbin and F. Hillion, J. Mater. Res. 7 (1992) 68.
[16] M.M. Waite and S.I. Shah, Appl. Phys. Lett. 60 (1992) 2344.
[17] P.A. Dennig and D.A. Stevenson, Appl. Phys. Lett. 59 (1991) 1562.
[18] D.N. Belton, S.J. Harris, S.J. Schmieg, A.M. Welner and T.A. Perry, Appl. Phys. Lett. 54 (1989) 416.
[19] W.A. Yarbrough, Science 247 (1990) 688.
[20] M. Tomellini and M. Fanfoni, Surf. Sci. 349 (1996) L191.
[21] L. Robbin Martin, J. Appl. Phys. 70 (1991) 5667.
[22] E. Molinari, R. Polini, M.L. Terranova, P. Ascarelli and S. Fontana, J. Mater. Res. 7 (1992) 1778.
[23] J. Rankin, R.E. Boekenhauer, R. Csencsits, Y. Shigesato, M.W. Jacobson and B.W. Sheldon, J. Mater. Res. 9 (1994) 2164.
[24] M. Tomellini, R. Polini and V. Sessa, J. Appl. Phys. 70 (1991) 7573.
[25] E. Molinari, R. Polini and M. Tomellini, J. Mater. Res. 8 (1993) 798.
[26] R. Polini and M. Tomellini, Diamond Relat. Mater. 4 (1995) 1311.
[27] M. Avrami, J. Chem. Phys. 7 (1939) 1103; 8 (1940) 212.
[28] K.K. Hirakuri, N. Mutsukura and Y. Machi, J. Appl. Phys. 78 (1995) 6520.
[29] R. Polini, J. Appl. Phys. 72 (1992) 2517.
[30] R.M. Feenstra and P. Martensson, Phys. Rev. Lett. 61 (1988) 447.
[31] B.M. Trafas, Y.N. Yang, R.L. Siefert and J.H. Weaver, Phys. Rev. B 43 (1991) 14107; F. Arciprete, S. Colonna, M. Fanfoni, F. Patella and A. Balzarotti, Phys. Rev. B 53 (1996) 12948.
[32] H. Brune, H. Röder, C. Boragno and K. Kern, Phys. Rev. Lett. 73 (1994) 1955.